Modeled spectral optical properties for smoke aerosols in Amazonia

A. S. Procopio
Universidade de São Paulo, Departamento de Física Aplicada, São Paulo, Brazil

L. A. Remer
NASA/GSFC, Laboratory for Atmospheres, Greenbelt, Maryland, USA

P. Artaxo
Universidade de São Paulo, Departamento de Física Aplicada, São Paulo, Brazil

Y. J. Kaufman
NASA/GSFC, Laboratory for Atmospheres, Greenbelt, Maryland, USA

B. N. Holben
NASA/GSFC, Laboratory for Terrestrial Physics, Greenbelt, Maryland, USA

Received 27 June 2003; revised 11 September 2003; accepted 14 October 2003; published 23 December 2003.

[1] The optical properties of aerosols from biomass burning in Brazil were derived from measurements by the AERONET sun photometer network in Amazonia. A dynamical aerosol model was constructed from Mie Theory calculations, using as input a constant complex refractive index and the average size distribution of aerosols for 12 ranges of aerosol optical thickness. The aerosol optical properties were described for 24 wavelengths in the spectral range of 0.20–3.00 μm. The model was used to simulate radiances and irradiances and the results agreed well with the measurements. The derived optical model is immediately applicable to estimate aerosol forcing by biomass burning aerosol emitted on the development frontier in Amazonia. *INDEX TERMS:* 0305 Atmospheric Composition and Structure: Aerosols and particles (0345, 4801); 3367 Meteorology and Atmospheric Dynamics: Theoretical modeling; 3359 Meteorology and Atmospheric Dynamics: Radiative processes; 9360 Information Related to Geographic Region: South America. **Citation:** Procopio, A. S., L. A. Remer, P. Artaxo, Y. J. Kaufman, and B. N. Holben, Modeled spectral optical properties for smoke aerosols in Amazonia, *Geophys. Res. Lett.*, *30*(24), 2265, doi:10.1029/2003GL018063, 2003.

1. Introduction

[2] Every year during the dry season in Amazonia satellites detect thousands of hot spots representing active man-made fires. Depending on the regional circulation and on the amount of fire activity, the smoke originating from fires in this Brazilian region can cover an area of 2–6 millions km^2, roughly up to half the size of the South American continent [*Prins et al.*, 1998]. The dry season begins in different months in Amazonia, mainly due to the seasonal migration of the Bolivian High and the ITCZ (intertropical convergence zone), but its peak occurs from August to November.

[3] Because of its large spatial and temporal extent, the biomass burning smoke represents a significant anthropogenic alteration of the natural environment, and becomes an important component in the energy balance, hydrological cycle and ecological systems of the region. Depending on the absorbing properties of the aerosols the smoke can warm the atmosphere while cooling the surface [*Kaufman et al.*, 2002]. This differential heating in the vertical column depends on the optical properties of the smoke particles and affects surface and column temperatures, the surface fluxes of sensible and latent heat, convection, cloud formation and precipitation [*Yu et al.*, 2003; *Ichoku et al.*, 2003]. Thus, an accurate aerosol model of the smoke optical properties is a necessary starting point in order to estimate the anthropogenic effects in Amazonia. However, the optical properties of smoke are not static, but vary with age of the smoke, type of material burned and size distribution [*Dubovik et al.*, 2002; *Holben et al.*, 1996]. A static aerosol model representing all smoke particles is simply inadequate.

[4] The objective of this study is to develop a dynamic aerosol model from volume size distributions inverted from sky radiance data obtained from sun photometers in Brazil during the dry season. A detailed characterization of the smoke optical properties can narrow the uncertainties on the estimations of the aerosol radiative forcing, and may possibly provide a way to better understand the ecosystem functioning under anthropogenic influences.

2. Input Data and Calculation

[5] The dynamic aerosol model was developed from measurements obtained during the dry seasons of 1999, 2000 and 2001 from two AERONET sun photometers [*Holben et al.*, 1998] located 700 km apart in the southern Amazon Basin, in the sites named Alta Floresta (09°55′S, 56°00′W) and Abracos Hill (10°45′S, 62°21′W). These instruments measure direct sun radiance that is converted to aerosol optical thickness (τ_a) in 7 wavelengths and also sky radiance at many angles that is inverted to retrieve aerosol volume size distribution, refractive indices and single scattering albedo [*Dubovik and King*, 2000]. This region is situated along the development frontier in the Amazon Region, also known as the Arch of Deforestation,

0094-8276/03/2003GL018063$05.00

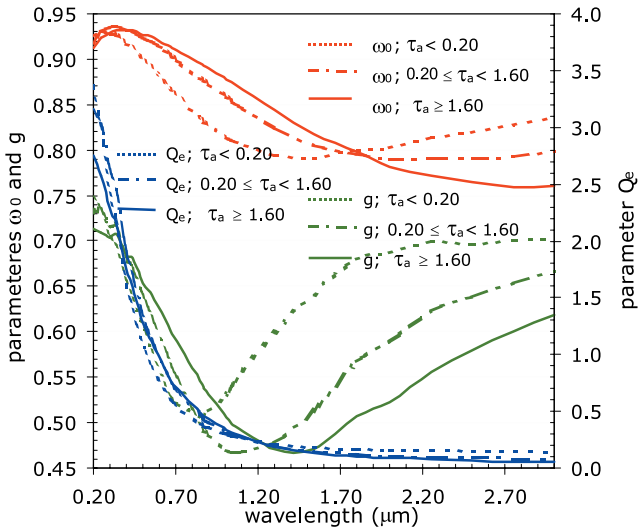

Figure 1. Spectral smoke aerosol optical properties as a function of aerosol optical thickness at 500 nm (τ_a) calculated from three years of data collected during the dry season in Amazonia. The red curves represent the single scattering albedo (ω_0), the green curves represent the asymmetry factor (g) and the blue curves represent the extinction efficiency (Q_e). Dotted curves refer to τ_a smaller than 0.20, dashed curves refer to τ_a between 0.20 and 1.60 and solid curves refer to τ_a greater than 1.60.

heavily impacted by biomass burning emissions and deforestation. The particles observed in this region are a combination of smoke emitted from burning of cerrado vegetation, pasture and primary and secondary forest [*Artaxo et al.*, 1998]. Over a region with the same type of chemical species, as the tropical forest, fires tend to have a typical average emission factor [*Andreae and Merlet*, 2001]. The AERONET retrievals characterize the local fresh fire emissions in the lower troposphere, as well as the aged pyrogenic pollutants in the upper troposphere, transported into it on a regional scale by deep convection [*Andreae et al.*, 2001; *Freitas et al.*, 2000].

[6] The AERONET climatology showed the range of τ_a (at 500 nm) at Alta Floresta and Abracos Hill to vary between 0.10 and 4.0 during the dry season, with the lower limit of 0.10 representing typical wet season values as well. The aerosol optical properties are expected to change as a function of τ_a [*Dubovik et al.*, 2002], and thus the aerosol model was designed to vary for different aerosol loading in the troposphere. The optical properties were determined for 12 situations that vary as a function of τ_a (at 500 nm): $\tau_a \leq 0.20$, $0.20 < \tau_a \leq 0.30$, $0.30 < \tau_a \leq 0.40$, $0.40 < \tau_a \leq 0.50$, $0.50 < \tau_a \leq 0.60$, $0.60 < \tau_a \leq 0.70$, $0.70 < \tau_a \leq 0.80$, $0.80 < \tau_a \leq 0.90$, $0.90 < \tau_a \leq 1.00$, $1.00 < \tau_a \leq 1.20$, $1.20 < \tau_a \leq 1.60$ and $\tau_a > 1.60$.

[7] A database of 517 volume size distributions obtained from AERONET [*Dubovik et al.*, 2000] were sorted as a function of τ_a (at 500 nm), separated into 12 cases, and for each case the mean size distribution was calculated [see supporting online material[1]]. These size distributions, derived from remote sensing data, refer to an atmospheric cross-section, requiring the assumption of a scale height in order to obtain a volume size distribution per unit of volume of air. Based on observations of the convective boundary layer height over pasture and forest in this region [*Nobre et al.*, 1996], the mean value of 1.6 km was assumed, not affecting the intrinsic optical properties of the particles. The total particle number concentration in the mean distributions varied from 3,100 #cm^{-3} to 34,200 #cm^{-3}, in agreement with measurements made by *Artaxo et al.* [2002], that found an average of 8,045 #cm^{-3}, with peaks reaching above 40,000 #cm^{-3}.

[8] The same database also provides complex refractive indices (m). The average and sample standard deviations of m of all data from the studied period were 1.50 ± 0.07 and 0.012 ± 0.006, for real (n) and imaginary (k) refractive indices respectively, in the wavelength range of 440–1020 nm. The large sample standard deviations reflect the natural variability of the system and not an inaccuracy of the measurements. *Dubovik et al.* [2002] found averages of $m = 1.47 - 0.00093i$ for Amazonian Forest and $m = 1.52 - 0.015i$ for Brazilian Cerrado. *Yamasoe et al.* [1998] found values ranging from 1.53 (440 nm) to 1.58 (1020 nm) for Brazilian Cerrado. *Remer et al.* [1998] assumed $m = 1.43 - 0.0035i$ in their calculations, before smoke measurements were available. The average value of m from our database ($1.50 - 0.012i$) was used to derive the aerosol model. This value was assumed to be constant across the entire range of τ_a and also constant spectrally.

[9] The main reason for this rationale is the availability of accurate AERONET size distribution data through the whole range of τ_a. The AERONET single scattering albedo (ω_0) and m retrievals are accurate only for τ_a (at 440 nm) greater than 0.40 [*Dubovik et al.*, 2000]. Besides, several analyses were done with the input data and the same degree of dependence was found between $\tau_a > 0.40$ and each of the parameters: n, ω_0 and ratio of fine to total modes. No significant relationship was found between k and τ_a. In contrast, an analysis between the whole range of τ_a and the ratio of fine to total modes showed that the correlation between these two parameters is twice stronger than that found with $\tau_a > 0.40$, and that most of their dependence occurs at $0.2 < \tau_a < 0.8$.

[10] The aerosol optical properties were calculated using the mean size distributions for each of the 12 cases with the average value of m, all determined from observations. A Mie calculation was used, assuming the particles to be spherical, which is acceptable for particles from smoldering combustion and aged smoke particles [*Martins et al.*, 1998].

3. Results

[11] The spectral modeled single scattering albedo (ω_0), asymmetry factor (g) and extinction efficiency (Q_e) for each one of the 12 cases studied were calculated and are shown in the supporting online material. These optical properties are plotted against wavelength in Figure 1 for the mean, lower and upper limits of τ_a. A ω_0 spectral dependence is seen, with the highest value (~0.92) in the ultraviolet and visible regions and the lowest (~0.78) in the mid-infrared region, as expected from Mie scattering. There was also an

[1]Auxiliary material is available at ftp://ftp.agu.org/apend/gl/2003GL018063.

Table 1. Comparisons of Single Scattering Albedo (ω_0), Asymmetry Factor (g) and Backscatter Fraction[a] (β) Calculated for Smoke Aerosols From Amazonia and Africa by Different Authors

	440 nm	670 nm	870 nm	1020 nm	
$\omega_0(\lambda)$[b]	0.93 ± 0.01	0.90 ± 0.01	0.87 ± 0.02	0.85 ± 0.02	average of the 12 cases, this work
	0.90	0.90	0.90	0.90	*Remer et al.* [1998] and *Kaufman et al.* [1992] (Amazonia)
	0.91 ± 0.03	0.89 ± 0.03	0.87 ± 0.03	0.85 ± 0.03	*Dubovik et al.* [2002] (Amazonia)
	0.86 ± 0.04[c] (Alta Floresta), 0.87 ± 0.03[c] (Abracos Hill)				*Schafer et al.* [2002] (Amazonia)
	0.88 ± 0.05[d]				*Eck et al.* [1998] (Amazonia)
	0.75 ± 0.10[d]				*Reid and Hobbs* [1998] (Amazonia)
	0.88 ± 0.02	0.84 ± 0.02	0.80 ± 0.02	0.78 ± 0.02	*Dubovik et al.* [2002] (Africa)
	0.90	0.87	0.85	0.82	*Haywood et al.* [2003] (Africa)
		0.79 ± 0.03[c]			*Schafer et al.* [2002] (Africa)
	0.90 to 0.85[e]	0.60			*Bergstrom et al.* [2003] (Africa)
$g(\lambda)$[b]	0.67 ± 0.01	0.56 ± 0.02	0.50 ± 0.02	0.48 ± 0.03	average of the 12 cases, this work
	0.65 ± 0.04	0.57 ± 0.06	0.50 ± 0.06	0.45 ± 0.07	*Remer et al.* [1998] (Amazonia)
	0.67 ± 0.03	0.59 ± 0.03	0.55 ± 0.03	0.53 ± 0.03	*Dubovik et al.* [2002] (Amazonia)
	0.64 ± 0.06	0.53 ± 0.06	0.48 ± 0.06	0.47 ± 0.06	*Dubovik et al.* [2002] (Africa)
	0.57	0.57	0.57	0.57	*Haywood et al.* [2003] (Africa)
	0.60	0.60	0.60	0.60	*Bergstrom et al.* [2003] (Africa)
$\beta(\lambda)$[b]	0.24 ± 0.02	0.27 ± 0.02	0.31 ± 0.02	0.32 ± 0.02	average of the 12 cases, this work
	0.21 ± 0.01	0.25 ± 0.01	0.28 ± 0.01	0.29 ± 0.01	*Remer et al.* [1998] (Amazonia)
	0.21 ± 0.02[d]				*Reid and Hobbs* [1998] (Amazonia)

[a]After *Wiscombe and Grams* [1976].
[b]Values are accompanied by a sample standard deviation.
[c]From pyranometer measurements, integrated over the total spectrum.
[d]From Broadband PAR irradiance measurements.
[e]Values in the visible.

increase of ω_0 (i.e. a decrease in absorption) with increasing τ_a in the visible and near-IR parts of the spectrum. Note that both the real and imaginary parts of m are kept constant in the calculations and that for aerosol particles with radius on the order of 10^{-1} μm the scattered intensity is primarily dependent on particle size [*Liou*, 2002]. The number of particles in the fine mode increases from case 1 to 12, but the number of particles in the coarse mode remains basically constant, showing that the differences seen in the values of ω_0 from case to case are related with the change in fine mode particles. The spectral dependence of g is very strong, with g decreasing sharply from the ultra-violet to the visible regions, and then increasing slower through the infrared region. In the visible region of the spectrum g is higher for higher values of τ_a, meaning that the higher the value of τ_a, the more radiation is scattered in the forward direction. In the infrared region there is an inversion on this pattern and the dependence on size distribution is stronger.

[12] Table 1 compares the optical parameters from this work with previous studies by different authors for the Amazonian region, and a good agreement within them can be observed. A comparison with aerosols from Amazonia and Africa shows stronger wavelength dependence with higher aerosol absorption in the later.

4. Testing the Aerosol Model

[13] Sky radiance data at 675 nm measured in the backscattering direction during the study period by the two sun photometers were used to test model predictions. Downwelling radiance at a solar zenith angle of 60° and a scattering angle of 120° from 165 observations were plotted as a function of τ_a and compared with simulations (Figure 2), calculated by means of a radiative transfer code for vegetated surface [*Ricchiazzi et al.*, 1998] using the smoke optical properties discussed on section 3. The modeled radiances represent mean conditions all through the τ_a range. Sensitivity to variations in ω_0 was also presented in this figure, showing the strong sensitivity to aerosol absorption. Surprisingly, the *Remer et al.* [1998] optical properties also represent the downwelling radiance, despite their differences in size distributions. The current model and the *Remer et al.* [1998] model do differ by 5% at higher τ_a where there is the greatest difference in size distribution. The reason for the general similarity in results is because both dynamic models have similar absorption at this wave-

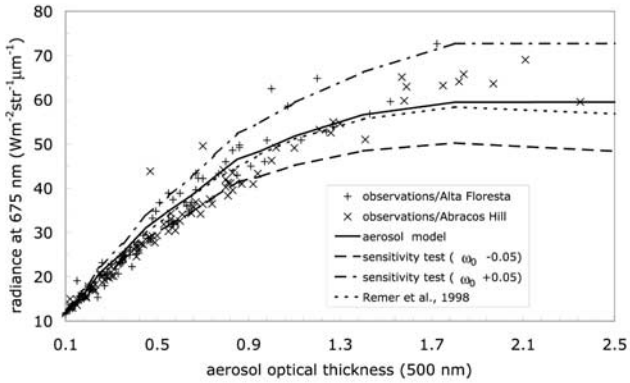

Figure 2. Downward radiance at 675 nm for a scattering angle of 120° and a solar zenith angle of 60° as a function of aerosol optical thickness at 500 nm. The crosses indicate observations by AERONET sun photometers at Alta Floresta and Abracos Hill. The curves represent values calculated from our aerosol model [supporting online material], from *Remer et al.* [1998] model, and for two sensitivity tests to different values of single scattering albedo (ω_0) applied to our model.

length ($0.87 \leq \omega_0 \leq 0.91$ in this work and $\omega_0 = 0.90$ in *Remer et al.* [1998]).

[14] The aerosol model was also tested through a comparison of 116 measured and calculated instantaneous downward solar fluxes at the surface, for cloud free days in Alta Floresta and Abracos Hill. The measured fluxes were obtained with pyranometers collocated with the sun photometers, which measured radiation flux in the 0.3–2.8 μm spectral range. Aerosol optical thickness (500 nm) varied from 0.4 to 1.56, water vapor varied from 2.98 to 4.17 g.cm^{-2} and solar zenith angle varied from 0 to 86.5°. The difference between modeled and measured total downward solar flux at the surface ranged from 0–5%, not showing any correlation with τ_a and in good agreement with the accuracy of the pyranometer. This result also shows that the aerosol model can be used for different solar zenith angles at both locations, with no increase of the maximum error.

[15] To test the sensitivity of the assumption of a constant *m* an approximation of a spectrally variable *m* of a mixture of aerosols was calculated. The aerosol mixture was defined based on the dry season aerosol mass source apportionment at Amazonia shown by *Artaxo et al.* [1998]. The *m* of the mixture was calculated using the "Bruggeman mixing rule" [*Chýlek and Srivastava*, 1993]. A humidification factor of 1.1 [*Kotchenruther and Hobbs*, 1998] was applied to introduce the effects of humidity variations on the aerosol optical properties [*Shettle and Fenn*, 1979]. The spectrally varying *m* [supporting online material] calculated for the aerosol mixture is unrealistic for wavelengths greater than 2.6 μm and should not be taken as precise, due to many assumptions taken in the calculations. The objective, however, was to test how the calculated aerosol optical properties vary and how this variation would affect the solar downward flux at the surface. Radiative transfer calculations made with both constant ($1.50-0.012i$) and variable indices showed a maximum difference of ±5% at the total downward flux at the surface, which is small considering the difference between the two assumptions.

[16] The above analyses showed that the dynamic aerosol optical model could successfully predict radiances at a single wavelength as well as irradiances integrated over the solar spectrum.

5. Concluding Remarks

[17] A dynamic spectral smoke aerosol model as a function of aerosol optical thickness was developed from three years of retrieved optical properties during the dry season in Amazonia. The model consists of a set of single scattering albedo, asymmetry factor and extinction efficiency at 24 wavelengths (200–3000 nm), for 12 different aerosol optical thickness ranges. It was shown that the model robustly simulates both narrowband and broadband downwelling solar radiation at the surface. Previous analyses of smoke optical properties done with similar data sets from Amazonia presented the climatology of retrieved optical properties within the limited spectral range of the observations or integrated across a spectral range, without calculating the parameters needed as input for detailed flux calculations. The model developed in this work is immediately applicable for studies of the aerosol radiative forcing by biomass burning smoke emitted on the development frontier in Amazonia, that will narrow the uncertainties associated with estimation of the anthropogenic influence on the local ecosystem and global climate.

[18] **Acknowledgments.** We thank the AERONET site managers for establishing and maintaining the network instruments. A.S. Procópio thanks financial support from FAPESP and AEROCENTER (NASA/GSFC). P. Artaxo acknowledges support from the Millennium Institute program from MCT/CNPq/PADCT.

References

Andreae, M. O., and P. Merlet, Emissions of trace gases and aerosols from biomass burning, *Global Biogeochem. Cycles*, *15*, 955–966, 2001.

Andreae, M. O., et al., Transport of biomass burning smoke to the upper troposphere by deep convection in the equatorial region, *Geophys. Res. Lett.*, *28*(6), 951–954, 2001.

Artaxo, P., et al., Large-scale aerosol source apportionment in Amazônia, *J. Geophys. Res.*, *103*(D24), 31,837–31,847, 1998.

Artaxo, P., et al., Physical and chemical properties of aerosols in the wet and dry seasons in Rondônia, Amazônia, *J. Geophys. Res.*, *107*(D2), 8081, doi:10.1029/2001JD000666, 2002.

Bergstrom, R. W., et al., Estimates of the spectral single scattering albedo and aerosol radiative effects during SAFARI 2000, *J. Geophys. Res.*, *108*(D13), 8474, doi:10.1029/2002JD0002435, 2003.

Chýlek, P., and V. Srivastava, Dielectric constant of a composite inhomogeneous medium, *Physical Review B*, *27*(n8), 5098–5106, 1993.

Dubovik, O., and M. D. King, A flexible inversion algorithm for retrieval of aerosol optical properties from sun and sky radiance measurements, *J. Geophys. Res.*, *105*, 20,673–20,696, 2000.

Dubovik, O., et al., Accuracy assessments of aerosol optical properties derived from Aerosol Robotic Network (AERONET): Sun and sky radiance measurements, *J. Geophys. Res.*, *105*, 9791–9806, 2000.

Dubovik, O., et al., Variability of Absorption and Optical Properties of Key Aerosol Types Observed in Worldwide locations, *J. Atmos. Sci.*, *59*, 590–608, 2002.

Eck, T., et al., Measurements of irradiance attenuation and estimation of aerosol single scattering albedo for biomass burning aerosol in Amazonia, *J. Geophys. Res.*, *103*(D24), 31,865–31,878, 1998.

Freitas, S. R., et al., A convective kinematic trajectory technique for low-resolution atmospheric models, *J. Geophys. Res.*, *105*, 24,375–24,386, 2000.

Haywood, J. M., et al., Comparisons of aerosol size distribuitions, radiative properties, and optical depths determined by aircraft observations and Sun photometers during SAFARI 2000, *J. Geophys. Res.*, *108*(D13), 8471, doi:10.1029/2002JD002250, 2003.

Holben, B. N., et al., Effect of dry-season biomass burning on Amazon basin aerosol concentrations and optical properties, 1992–1994, *J. Geophys. Res.*, *101*(D14), 19,465–19,481, 1996.

Holben, B. N., et al., AERONET: A federated instrument network and data archive for aerosol characterization, *Remote Sensing Environment*, *66*, 1–16, 1998.

Ichoku, C., et al., MODIS observation of aerosols and estimation of aerosol radiative forcing over southern Africa during SAFARI 2000, *J. Geophys. Res.*, in press, 2003.

Kaufman, Y. J., et al., Biomass Burning Airborne and Spaceborne Experiment in the Amazonas (BASE-A), *J. Geophys. Res.*, *97*(D13), 14,581–14,599, 1992.

Kaufman, Y. J., D. Tanré, and O. Boucher, A satellite view of aerosols in the climate system, *Nature*, *419*, 215–223, 2002.

Kotchenruther, R., and P. V. Hobbs, Humidification factors of aerosol from biomass burning in Brazil, *J. Geophys. Res.*, *103*(D24), 32,081–32,089, 1998.

Liou, K. N., *An Introduction to Atmospheric Radiation*, Second Edition, Academic, USA, 2002.

Martins, J. V., et al., Sphericity and morphology of smoke from biomass burning in Brazil, *J. Geophys. Res.*, *103*(D24), 32,051–32,057, 1998.

Nobre, C. A., et al., "Observations of the atmospheric boundary layer in Rondônia" in *Amazonian Deforestation and Climate*, edited by J. H. C. Gash et al. (eds), chapter 24, John Wiley and Sons, 1996.

Prins, E. M., et al., An overview of GOES-8 diurnal fire and smoke results for SCAR-B and 1995 fire season in South America, *J. Geophys. Res.*, *103*(D24), 31,821–31,835, 1998.

Reid, J. S., and P. V. Hobbs, Physical and optical properties of young smoke from individual biomass fires in Brazil, *J. Geophys. Res.*, *103*(D24), 32,013–32,030, 1998.

Remer, L. A., et al., Biomass burning aerosol size distribution and modeled optical properties, *J. Geophys. Res.*, *103*(D24), 31,879–31,892, 1998.

Ricchiazzi, P., et al., SBDART: A Research and Teaching Software Tool for Plane-Parallel Radiative Transfer in the earth's Atmosphere, *Bull. Am. Meteorol. Soc.*, *79*, 2101–2114, 1998.

Schafer, J. S., et al., Observed reductions of total solar irradiance by biomass burning aerosols in the Brazilian Amazon and Zambian Savanna, *Geophys. Res. Lett.*, *29*(17), 1823, doi:10.1029/2001GL014309, 2002.

Shettle, E. P., and R. W. Fenn, *Models for the aerosol of the lower atmosphere and the effects of humidity on their optical properties*, Air Force Geophysics Laboratory Report, Hanscom Air Force Base, MA, USA Dept. of Commerce, 1979.

Wiscombe, W. J., and G. W. Grams, The backscattered fraction in two-stream approximations, *J. Atmos. Sci.*, *33*, 2440–2451, 1976.

Yamasoe, M. A., et al., Retrieval of the real part of the refractive index of smoke particles from sun/sky measurements during SCAR-B, *J. Geophys. Res.*, *103*(D24), 31,893–31,902, 1998.

Yu, H., S. C. Liu, and R. E. Dickinson, Radiative effects of aerosol on the evolution of the atmospheric boundary layer, *J. Geophys. Res.*, *107*, doi:10.1029/2001JD000754, 2003.

A. S. Procopio and P. Artaxo, Instituto de Física, Universidade de São Paulo, Rua do Matão, Travessa R, 187, São Paulo, 05508-900, Brazil. (aline@if.usp.br)

B. N. Holben, NASA Goddard Space Flight Center, Laboratory for Terrestrial Physics, code 923, Greenbelt, MD 20771, USA.

L. A. Remer and Y. J. Kaufman, NASA Goddard Space Flight Center, Laboratory for Atmospheres, code 913, Greenbelt, MD 20771, USA.